



Contents lists available at ScienceDirect

# Journal of Electron Spectroscopy and Related Phenomena

journal homepage: [www.elsevier.com/locate/elspec](http://www.elsevier.com/locate/elspec)

## Approaches to analyzing insulators with Auger electron spectroscopy: Update and overview

D.R. Baer<sup>a,\*</sup>, A.S. Lea<sup>a</sup>, J.D. Geller<sup>b</sup>, J.S. Hammond<sup>c</sup>, L. Kover<sup>d</sup>, C.J. Powell<sup>e</sup>, M.P. Seah<sup>f</sup>, M. Suzuki<sup>g</sup>, J.F. Watts<sup>h</sup>, J. Wolstenholme<sup>i</sup>

<sup>a</sup> Environmental Molecular Sciences Laboratory, Pacific Northwest National Laboratory, Richland, WA 99352, USA

<sup>b</sup> Geller MicroAnalytical Laboratory, Topsfield, MA 01983-1216, USA

<sup>c</sup> Physical Electronics Inc., Chanhassen, MN 55317, USA

<sup>d</sup> Institute of Nuclear Research of the Hungarian Academy of Sciences (ATOMKI) Debrecen, H-4026 Hungary

<sup>e</sup> National Institute of Standards and Technology, Gaithersburg, MD 20899-8370, USA

<sup>f</sup> National Physical Laboratory, Teddington TW11 0LW, United Kingdom

<sup>g</sup> ULVAC-PHI Inc., Chigasaki, Kanagawa 253-8522, Japan

<sup>h</sup> University of Surrey, Guildford, Surrey GU2 7XH, England

<sup>i</sup> Thermo Fisher Scientific, East Grinstead, West Sussex RH19 1UB, United Kingdom

### ARTICLE INFO

#### Article history:

Available online 7 April 2009

#### Keywords:

Auger electron spectroscopy  
Surface charging  
Surface analysis  
Practical guide

### ABSTRACT

This paper provides an updated overview, intended to be of practical value to analysts, of methods that can be applied to minimize or control the build-up of near-surface electrical charge during electron-induced Auger electron spectroscopy (AES). Although well-developed methods can be highly effective, dealing with insulating or ungrounded samples for which high spatial resolution is needed remains a challenge. Examples of the application of methods involving low-energy ion sources and sample thinning using a focused ion beam that can allow high-resolution measurements on a variety of samples are highlighted. The physical bases of newer and traditional methods are simply described along with strengths and limitations of the methods. Summary tables indicate methods that can be applied to most AES spectrometers, methods that require special instrumental capabilities and methods that require special sample preparation or mounting.

© 2009 Elsevier B.V. All rights reserved.

### 1. Introduction

The composition and chemical state of surfaces and interfaces strongly influence many properties of both natural (e.g., aerosols, particles, particulates, and mineral phases) and man-made materials (e.g., catalysts, electronic components, carbon nanotubes (CNTs)). It is increasingly important to understand the full complexity of many natural systems and to characterize the complexities that can now be designed into a wide variety of synthetic structures, including nanometer-sized features. Electron-beam-based methods including scanning electron microscopy (SEM) and transmission electron microscopy (TEM) are essential tools for obtaining structural information down to the nanometer dimensions. Electron-beam-based Auger electron spectroscopy (AES) is often used to obtain elemental (and sometimes chemical state) information about surfaces and small particles.

Although electron-beam methods offer the advantage of high spatial resolution, there can be important complications due to charge accumulation on or near the sample surface which can alter or make the sample surface potential unstable (causing shifting peaks, arcing, etc.) significantly diminishing the quality of images, changing the apparent energy and/or intensity of Auger electrons, shifting the location of the probing beam, and frequently altering the sample composition or structure (damage). Sample charging issues are well known in electron microscopy and there are a variety of methods to check for their presence or to minimize their effects. Although many of the physical processes producing charging are common for SEM, TEM and AES and many of the solutions are similar [1,2], not all of the standard microscopy tools apply to AES because of the energies involved in collecting an AES spectrum and the surface sensitivity of AES signals. Stability and analysis issues are particularly challenging for analysis of many modern materials for which high-spatial-resolution surface and near-surface analysis would be particularly useful, including materials that are highly insulating (such as modern multi-phase ceramics) and systems that mix insulating and conducting components (including modern semiconductor structures).

\* Corresponding author. Tel.: +1 509 371 6245; fax: +1 509 371 6242.  
E-mail address: [don.baer@pnl.gov](mailto:don.baer@pnl.gov) (D.R. Baer).

Because of the increased technological importance of surface analysis, Technical Committee (TC) 201 on Surface Chemical Analysis of the International Organization for Standardization (ISO) and ASTM International's, Committee E-42 on Surface Analysis have developed a series of standards and recommended practices. During development of a new ISO standard "Surface Chemical Analysis – Auger electron spectroscopy – Reporting of methods used for charge control and charge correction" ISO 29081, it became clear that although the theoretical understanding of surface charging was well established [3,4] many excellent reviews had been published [5–8] and a variety of new approaches had been developed [9–12] or facilitated by instrumental advances, there was no up to date practical reference or guide for analysts that integrated newer and more traditional approaches for controlling charging during AES analysis. Some of the information obtained during the development of the ISO standard is therefore included in this paper and the authors of this paper include international experts who helped develop an informative annex of the ISO standard. The objective of this review is to provide an easily accessible guide and framework to assist analysts in dealing with charging during electron-generated AES. Analysts are encouraged to use ISO 29081 for reporting the methods they use to address charging during AES analysis. Other relevant ASTM and ISO standards and guides include those involving specimen handling [13,14] and a guide for "Minimizing Unwanted Electron Beam Effects in Auger Electron Spectroscopy" [15].

Charging of insulators has been an important issue or complication for AES and the related surface-sensitive technique of X-ray photoelectron spectroscopy (XPS) since AES and XPS were developed. Whereas major advancements in dealing with charging for XPS appeared in the late 1990s, "less progress has been made in analysis of such samples with AES, which remains a challenging task in many cases" [7]. A wide variety of approaches for dealing with charging during AES have been used over time with varying degrees of success. The development of additional tools started appearing in the patent literature in the late 1980s and, with advances in instrumentation, these and other approaches began to be applied and appear in journal articles in the late 1990s and early 2000s. These methods include specialized sample preparation, sometimes involving newly developed capabilities, and increased application of low-energy ions to assist charge compensation. Nonetheless, no single method has been found to overcome all charging problems during AES analysis [5,7] and in some circumstances charging difficulties may be impossible to avoid.

Many of the approaches for dealing with charging (see Tables 3–5) are summarized in this overview and discussed with a short description of the physical basis or objective of the method. As examples of application of newer tools, the use of low-energy (<50 eV) ions now available from some ion guns and the use of a focused ion beam (FIB) to minimize changes in the sample potential will be presented along with discussion of the advantages and limitations of the methods. This paper focuses on practical aspects of AES analysis while a more detailed mechanistic description, especially related to secondary electron emission, is provided by Cazaux [16] included in this special issue of the Journal of Electron Spectroscopy and Related Phenomena on Charging Effects in Electron Spectroscopies.

## 2. Charge build-up during AES

Relatively high spatial resolution (in three dimensions) for the determination of chemical composition is a major strength of AES. Depending upon the specific experimental system, the spatial resolution for AES can be characterized by an information depth of  $\approx 10$  nm, a lateral resolution down to  $\approx 10$ – $20$  nm, and a depth reso-

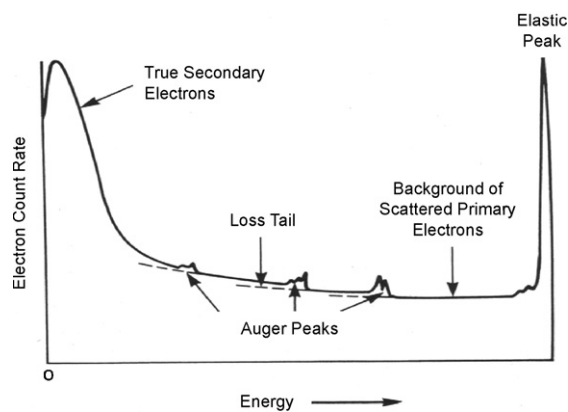


**Fig. 1.** Schematic representation of an Auger spectrum showing the full range and energy distribution of electrons leaving a sample and being detected from a sample being irradiated by an electron beam. An elastic peak from the primary beam, true secondary electrons (<50 eV) and Auger peaks are shown. Also shown are the background of scattered primary electrons and loss tail contributions to the background from each Auger peak. All of these electrons contribute to the total secondary electron yield (TSEY). After Strausser [17].

lution of  $\approx 1$  nm. Although the information depth of Auger electrons is  $\approx 10$  nm, the penetration depth of the incident electron beam is considerably deeper. The incident electron beam initiates many different processes in the sample, in addition to the generation of Auger electrons. Electrons having a wide range of kinetic energy are emitted from the sample including electrons elastically backscattered from the primary beam, electrons from the primary beam that have been inelastically scattered (losing energy to the sample), Auger electrons, and secondary electrons produced by the decay of excitations induced by primary, scattered, and Auger electrons, as shown in Fig. 1 [17]. Depending on the total number of electrons arriving and departing, the electrical potential of the sample may be altered due to charge build-up at the sample surface and in the sub-surface region (to the depth of the penetrating electrons) for materials that do not have the ability to discharge electrons to ground. In addition to impacting the ability to generate and collect Auger electrons, charge build-up may also initiate processes that can alter the composition near the surface of the sample.

The amount and distribution of surface and near-surface charge in a specific sample will be influenced by many sample and instrument factors including primary beam energy, primary current density, incidence angle of the beam on the sample, specimen composition, specimen homogeneity, surface contamination (including dust particles on a surface), magnitude of bulk and surface conductivities, surface topography, the vacuum environment, the presence of neutralizing low-energy electrons or ions, and the accumulation of charge on insulating materials near the sample. Charge build-up often occurs both along the sample surface and into the material [18]. The presence of particles or different phases on or within a specimen may contribute to an uneven distribution of charge across the surface and within the sample, a phenomenon known as differential charging. Charge build-up may also occur at phase boundaries, interface regions or defects within the sample. Insulating specimens undergo time-dependent changes in the amount of charging because of charge accumulation within the material and/or because of chemical and physical changes induced by primary or secondary electrons (including electron-stimulated desorption [5,7], electron-induced sputtering [19] and electron-induced adsorption) or specimen heating.

The essence of charging is the accumulation of charge near the surface of the sample that alters the electrical potential. When large enough, this potential alters the energy and intensity of Auger electrons, creates a field that changes the location at which the

primary beam strikes the specimen, and may change the near-surface composition of the sample and lead to arcing and localized sample breakdown. There is little charge build-up on any sample with low resistivity that is properly grounded. Even many samples thought to have a moderate to relatively high resistivity may not charge significantly for AES. For these cases, the sample may be thought of as a simple resistor. In contrast, the appropriate model for a highly insulating sample, or parts of a sample isolated from ground, is that of a capacitor, or possibly a leaky capacitor. A conceptual overview of factors contributing to sample charging including specimen resistivity, sample capacitance, the secondary-electron yield and time-dependent phenomena is presented in the following section. The discussion is not comprehensive, but is intended to provide a framework for describing approaches used to address charging in AES. It should be remembered that, even if a surface potential is controlled, there will be a sub-surface distribution of charges that may affect the backscattering, cause sample modification (damage) or influence other sample properties.

### 2.1. Factors influencing surface potential

The charge build-up on insulators due to incident electron beams has been examined for many years. A simple way to estimate the sample resistance that would induce sample charging has been presented by Hofmann [5]. Using the assumption that 1 V of charging is acceptable for AES analysis (i.e., an energy shift of 1 eV), Hofmann showed that many resistive materials have sufficient conductivity to allow for typical AES analyses with little charging. Hofmann estimated conditions when charging might exceed 1 V using a version of Ohm's law. The surface potential ( $U_s$ ) of a resistive specimen on a conducting substrate was approximated by

$$U_s \approx \rho z j_p (1 - \sigma) \quad (1)$$

where  $\rho$  is the electrical resistivity of the sample,  $z$  is the sample thickness,  $j_p$  is the incident (primary) electron current density and  $\sigma$  is the total secondary-electron yield (TSEY). The TSEY is the ratio of the total number of electrons emitted from a sample to the total number of electrons incident at a given energy and angle of incidence. By convention, the TSEY is the sum of the "true" secondary-electron yield  $\delta$  arising from emitted electrons with energies  $\leq 50$  eV and the yield of backscattered electrons  $\eta$  arising from electrons with energies larger than 50 eV. Many experimental and theoretical studies have been made of the TSEY [4,16], and some important elements of this work will be discussed in a later section.

If the incident or primary beam current is  $I_p$  and the secondary-electron current is  $I_s$ ,  $\sigma = I_s/I_p$ . Using Eq. (1), an assumed sample thickness of 1 mm and, for simplicity, that  $\sigma = 0$  (which is never true), Hofmann [5] showed that many relatively highly resistive materials are sufficiently conducting for typical AES analyses. However, the needed conductivity is highly sensitive to the beam current density, sample size, and geometry (especially thickness). The conductivity requirements for highly focused electron beams can differ by  $10^6$  when compared to a large-area analysis (which would be possible for a uniform material). As one specific example, a potential of 1 V or less will occur for a 10 nA beam defocused into an area of  $1 \mu\text{m}^2$  for any 1 mm thick sample with a resistivity of  $0.1 \Omega\text{m}$  or less. These conditions change for thicker (or thinner) samples and also depend on the beam current and beam area. Typical values of resistivity for some common materials are shown in Table 1 [20]. To enable simple comparison of the resistivity of a specific material with that of a good conductor, the ratio of the resistivity of each material to that of copper is also listed. Examples of different electron beam conditions, related current densities and "threshold" conductivities calculated from Eq. (1) assuming  $\sigma = 0$  and a 1 mm thick sample are shown in Table 2.

**Table 1**

Typical values of the bulk resistivity of selected classes of materials and the ratio of those resistivity values to the resistivity of copper [20].

Material	Resistivity ( $\Omega\text{m}$ )	Ratio of resistivity to resistivity of Cu [ $\rho_{\text{Cu}} \sim 10^{-8} \Omega\text{m}$ ]
Metals	$10^{-8}$ to $10^{-6}$	1 to $10^2$
Semiconductors	$10^{-5}$ to $10^5$	$10^3$ to $10^{13}$
Ge	1	$10^8$
Si	$10^{-3}$	$10^{11}$
Ceramics (insulators)	$10^6$ to $10^{14}$	$10^{14}$ to $10^{22}$
Carbides		
$\text{B}_4\text{C}$	$10^{-2}$	$10^6$
NbC	$10^{-7}$	$10^1$
SiC	$10^{-3}$	$10^5$
TiC	$10^{-6}$	$10^2$
ZrC	$10^{-6}$	$10^2$
Diamond	$10^{10}$ to $10^{11}$	$10^{18}$ to $10^{19}$
Graphite	$10^{-6}$	$10^2$
Oxides		
$\text{Al}_2\text{O}_3$	$10^{12}$ to $10^{14}$	$10^{20}$ to $10^{22}$
$\text{Fe}_3\text{O}_4$	$10^{-1}$	$10^7$
$\alpha\text{-Fe}_2\text{O}_3$ Film	$10^4$	$10^{12}$
MgO	$10^4$	$10^{12}$
ZnO	$10^8$	$10^{16}$
$\text{ZrO}_2$	$10^8$	$10^{16}$
Glasses	$10^9$ to $10^{14}$	$10^{17}$ to $10^{22}$
Pyrex	$10^{16}$	$10^{24}$
Soda	$10^{13}$	$10^{21}$
Quartz	$10^{12}$ to $10^{16}$	$10^{20}$ to $10^{24}$
Fused silica	$10^{18}$	$10^{26}$
Nitrides		
AlN	$10^7$	$10^{15}$
CrN	$10^{-4}$	$10^4$
NbN	$10^{-6}$	$10^2$
$\text{Si}_3\text{N}_4$	$10^{10}$	$10^{18}$
TiN	$10^{-7}$	$10^1$
Polymers	$10^6$ to $10^{19}$	$10^{14}$ to $10^{27}$
Bakelite	$10^{11}$	$10^{19}$
Poly(acetylene) (undoped)	$10^6$	$10^{14}$
Poly(vinyl chloride)	$10^{15}$	$10^{23}$
Teflon	$10^{16}$	$10^{24}$

Although Eq. (1) provides information about the lower level of sample resistivity that might make a specimen susceptible to charging, it is based on a highly simplified view of a complex problem. The equation cannot predict, for example, the very high surface potentials that can form on highly insulating materials where an issue of particular importance is the nature and variability (including changes due to surface charging) of the TSEY [3].

**Table 2**

Rough estimates for lower limits of resistivity thresholds for possible charging problems during AES for different electron-beam conditions. Calculations have been done for a 1 mm thick sample. Resistivity values lower than those shown in column 2 are unlikely to produce significant charging. Based on a table by Hofman [5].

	Threshold resistivity ( $\Omega\text{m}$ )	Average current density ( $\text{A}/\text{m}^2$ )	Current ( $\mu\text{A}$ )	Beam diameter ( $\mu\text{m}$ )	Raster ( $\mu\text{m}$ )	Area ( $\mu\text{m}^2$ )
Large area	1.0E+03	1.0E+00	0.01	0.02	100 × 100	1.00E+04
	1.0E+01	1.0E+02	1	0.02	100 × 100	1.00E+04
	1.0E−01	1.0E+04	0.01	0.02	1 × 1	1.00E+00
	7.9E−02	1.3E+04	0.01	1.00	None	7.85E−01
	4.0E−03	2.5E+05	0.01	0.02	0.2 × 0.2	4.00E−02
7.9E−04	1.3E+06	1	1.00	None	7.85E−01	
Smallest spot	3.1E−05	3.2E+07	0.01	0.02	None	3.14E−04

For specimens that accumulate charge upon beam irradiation, it is appropriate to view the sample as a capacitor. In this case the surface potential is related to the charge  $Q$  per surface area  $S$  [ $Q/S$ ], the sample thickness ( $z$ ) and the dielectric constant  $\epsilon$  [1,3]

$$U_s \approx \frac{Q}{C} \approx \frac{Qz}{\epsilon S} \quad (2)$$

The net charge on the sample ( $Q$ ) will arise from an imbalance of the incident and outgoing electron currents (the TSEY  $\sigma$  includes contributions mainly from secondary and backscattered electrons since the contribution of Auger electrons is negligible). This imbalance may be positive or negative. Assuming no leakage (infinite resistivity), the change in charge accumulated on the sample ( $\partial Q/\partial t$ ) will be related to the TSEY through the following relation:

$$\frac{\partial Q}{\partial t} = I_p(1 - \sigma) \quad (3)$$

When  $\partial t$  is chosen to be  $t$  the radiation time,  $I_p t$  is the fluence (or dose) of the radiation.

It is important to recognize that the TSEY  $\sigma$  changes as charge accumulates during irradiation (or as the sample composition changes), and that Eq. (3) is only valid for excitation by short pulses of primary electrons. Consideration of the sample as a capacitor during AES, XPS and SEM analysis has been discussed in detail by Cazaux for both uniform large-beam irradiation and for focused-beam conditions [2–4].

Even a very cursory examination of Eqs. (1)–(3) provides some important general information related to controlling charging. First, methods that lower sample resistance to ground, minimize the net (total of positive and negative) current to the sample, optimize the secondary-electron yield, or increase sample capacitance may be useful approaches for minimizing charge build-up on the sample. Decreasing the thickness ( $z$ ) of a sample, for example, may lower the surface potential in both Eqs. (1) and (2), and thus be useful for many types of samples susceptible to charging. The time dependence introduced in Eq. (3) indicates that some behaviors will be time-dependent.

The TSEY ( $\sigma$ ) plays a very important role in charge balance and methods that influence the TSEY will provide useful approaches for minimizing charge accumulation, and some specific examples will be discussed later. At this point, it is relevant to highlight two important properties of the TSEY. First, the TSEY is angle and energy dependent as shown schematically in Fig. 2. Therefore, the energy and angle at which the primary beam strikes the surface will have a strong impact on the secondary-electron yield. A second property of

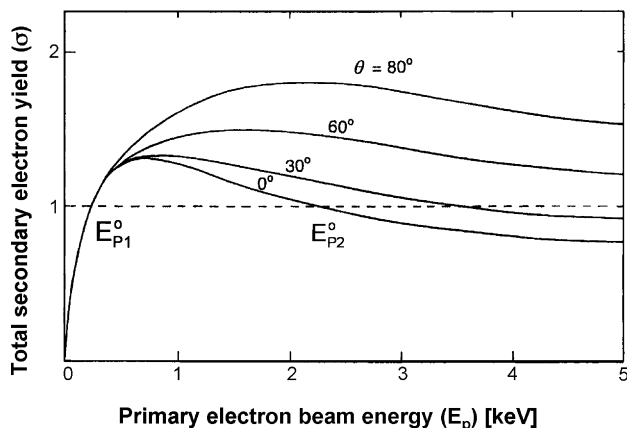


**Fig. 2.** Schematic plot of the total secondary-electron yield,  $\sigma$ , as a function of the energy of the primary-electron beam ( $E_p$  in keV) for four angles of incidence,  $\theta$ , with respect to the surface normal.  $E_{p1}^0$  and  $E_{p2}^0$  are the primary-electron beam energies for which  $\sigma = 1$ . After Seah and Spencer [21].

importance, already mentioned, is that the TSEY is time-dependent [3,16]. The TSEY changes as the sample accumulates charge at or near the surface. The sign and extent of the charge build-up over time is to a significant degree predictable and depends on the energy of the electron beam relative to two energies,  $E_{p1}^0$  and  $E_{p2}^0$  in Fig. 2 for which  $\sigma = 1$ . These critical energies are material and often time-dependent [3,21]. This second property again highlights the importance that the electron beam energy plays and provides a tool to minimize charging effects.

Most of the methods developed to minimize charging during AES can be divided into three categories: (i) those which decrease sample resistance to ground or increase capacitance; (ii) those which adjust or optimize the TSEY; and (iii) those which adjust the total current to the sample. Methods in these three areas are listed in Tables 3–5, respectively, and each of the identified topics will be briefly discussed below. As different approaches for minimizing charging (and sample damage) are considered, we will also note the relative ease with which specific methods can be implemented ('Ease of Application' column in these tables). Some methods can be applied to most samples in almost any spectrometer (routine operator control) while others require special capabilities within or outside the spectrometer and may involve special sample mounting or preparations. Other approaches may require low-energy primary-electron beams that will limit the achievable lateral resolution and may not be useful for specimens requiring analysis of small features. Some approaches are particularly useful for materials that have "marginal" conductivity for AES, but will be less successful for samples that have higher resistivity. An analyst must appropriately consider the analysis needs and what is known about the nature of the specimen material to determine which of these approaches is suitable for the analysis.

### 3. Recent developments

Before summarizing many of the approaches that can be used to minimize charging, it is useful to highlight recent developments or applications. Because many modern materials contain features with sizes on the order of a few to tens of nanometers, it is increasingly important to be able to obtain AES data with high lateral resolution on materials that may have a range of electrical conductivities or varying electrical connectivities to ground. Some recent developments are particularly oriented toward the ability to collect such data. Although not totally new, two approaches have been facilitated by technology advances that enable them to be applied more easily. These include the use of low-energy ions (to adjust the total current to the sample) and the application of focused ion beam (FIB) systems to thin samples (decreasing resistance to ground).

#### 3.1. Low-energy ions

The potential value of low-energy ion beams for charge neutralization was recognized many years ago. US Patent 4249077 was granted to C.K. Crawford of Kimball Physics in 1981; he proposed the use of low-kinetic-energy positive ions for charge neutralization. In the 1990s, Larson and Kelly [22] (US patent 5990476 and European Patent EP0848247) recognized that a combination of low-energy ions and low-energy electrons was useful for charge neutralization in XPS. This combination worked very well and manufacturers developed the ability to operate  $\text{Ar}^+$  ion guns used for ion sputtering at sufficiently low energies to facilitate charge neutralization. Over some time, the technology developed initially for XPS has been successfully implemented in commercial AES systems, thereby providing an enhanced ability to collect AES data on insulating samples. Currently, several manufacturers [23] of Auger electron spectrometry systems produce ion guns that can be used at voltages between

**Table 3**  
Methods for minimizing sample charging that effectively alter sample dimensions increasing capacitance or decreasing the overall resistance of the analysis area to ground.

Method	General Approach or objective	Type of sample	Ease of application	Refs.
Increasing electron beam energy	Minimizing resistance (MR) (creating conduction pathway through film)	Thin films on a conducting substrate through which a higher energy electron beam can penetrate	Routine operator control	[5,7,26]
Mounting sample on metal or conducting tape	MR (creating short pathway to ground)	Fine particles or powders	Mounting sample	[5,7,13,14,49]
Cover sample with conducting mask or grid	MR (creating short pathway to ground) or increasing capacitance	Bulk insulators, highly insulating films or marginally conducting materials	Mounting sample	[5,7,13,14,49]
Thinning sample	MR (decreasing effective sample thickness) or increasing capacitance	Bulk specimens thinned by a variety of methods including ion sputtering	Altering sample	[5,9,10,27,30]
Placing thinned samples on a low-atomic-number substrate	MR and enhanced spatial resolution by minimizing electron backscattering	Specimens that can be thinned by FIB or other precise method for which high-lateral resolution information is needed	Altering sample or sample design	[9,10]
Doping or processing sample	Decreasing sample resistivity (DSR)	Specimens that can be either doped during synthesis to increase conductivity or those for which processing can increase conductivity	Altering sample	[34,35]
Heating sample in spectrometer	DSR and/or detrapping trapped charge	Bulk samples or films that are stable upon heating and for which the resistivity lowers at moderate temperatures	Special capability	[5]

**Table 4**  
Methods for minimizing sample charging that are related to changing the secondary-electron yield.

Method	General Approach or Objective	Type of Sample	Ease of Application	Refs.
Adjusting electron beam energy	Enhancing secondary electron emission (ESEE) by matching electron penetration to secondary-electron escape distance	Bulk insulators or highly insulating films	Routine operator control	[4,7,8,42]
Tilting sample relative to electron beam	ESEE by matching electron penetration to secondary-electron escape distance	Bulk insulators or highly insulating films	Routine operator control	[4,5,7,8,21,42]
Cleaning sample	ESEE by removing contaminants to change secondary-electron yield, sometimes reducing charging (but sometimes increasing charging)	Bulk insulators or insulating films	Special capability or remounting sample	[40,41]

about 10 and 50V for charge neutralization during AES measurements [10–12].

The application of a low-energy ion beam during electron irradiation has been found to stabilize the surface potential and to enhance the uniformity of the potential on the surface. As an example of the impact of this approach, Fig. 3 shows AES spectra from an aluminum bond pad on an insulating substrate with and without the bombardment by 20 eV Ar<sup>+</sup> ions [12]. The spectrum collected with the ions restored the low energy Auger peaks and has the overall structure and AES peak shapes expected while without the ions the spectrum is highly distorted.

Because of potential sample modification or damage due to ion-surface interactions, the specific ion-beam energy and currents used are of importance. JEOL [23] reports that when ions of less than 20 eV are used, sputtering of SiO<sub>2</sub> is not observed [10]. A study on isolated bond pads with a Physical Electronics [23] 700 scanning AES system shows that, for a specific primary-beam energy, primary current, and geometrical conditions, a stable surface potential was achieved by bombarding the sample with 10 eV Ar<sup>+</sup> ions, as indi-

cated by condition 2 in Fig. 4 [11]. Operating conditions 1 and 3 in Fig. 4 are clearly less desirable.

The application of low-energy ions can help the analyst to obtain stable AES spectra, AES composition maps, and SEM images. Fig. 5 shows (a) an SEM image of a gold-plated bonding pad (examined in Fig. 4) and (b) a Ni Auger map that indicates Ni islands on the pad [11]. An overlay of N and O AES signals from a bulk ceramic sample is shown in Fig. 6 [12]. In the latter application, useful SEM and AES data could not be obtained without concurrent bombardment of the sample with 20 eV Ar<sup>+</sup> ions. Although the application of low-energy ions is not yet highly represented in the literature (in part due to the recent introduction of commercial ions guns with the low-energy capability) and may be, currently, as much an art as a science, the method appears to significantly extend the range of materials and materials systems for which AES data can be obtained with relatively high spatial resolution. Nevertheless, an analyst must remain aware of the possibility of sample damage by either the electrons or ions incident on the surface. In addition, while the low-energy ions can neutralize surface charge and reduce

**Table 5**  
Methods for minimizing sample charging that are associated with total sample current and charge accumulation<sup>a</sup>.

Method	General approach or objective	Type of sample	Ease of application	Refs.
Lowering beam current or current density	Minimize current (MC) through sample to lower $U_s$ or minimizing charge accumulation during analysis	High-resistance samples	Routine operator control	[4,5,7,21]
Gases added to vacuum system	Minimize damage and increase charge transport	Oxides (and possibly other dielectrics)	Special capability	[45]
Low-energy ion source	MC by charge compensation and creation of a more uniform surface potential	Bulk materials or mixed conducting and non-conducting phases	Special capability	[5,7,10,11,12]
Secondary-electron source	MC by establishing positive potential establishing self-compensation condition	Bulk insulators	Special capability	[5,6,7,42]
Minimizing total electron dose	Minimize charge accumulation and related potential-driven sample-composition changes	Dielectrics for which damage has been reported or observed	Routine operator control	[4,5,21]

<sup>a</sup> Items included in this table involve control of current to the sample and are listed here even if the intent of an extra current source is to influence the secondary electron yield.

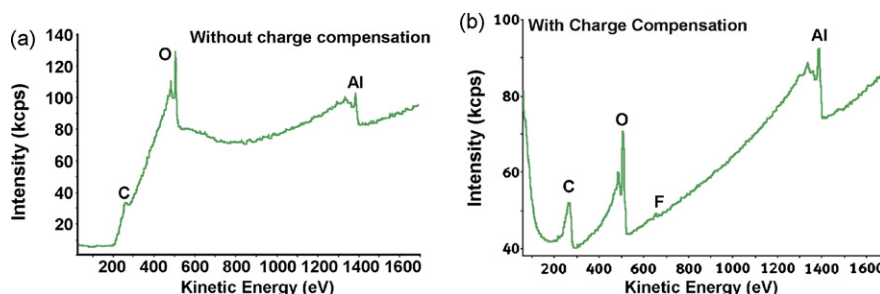


**Fig. 3.** AES spectra collected on a Thermo Electron MICROLAB 350 [23] from an aluminum bond pad on an insulating substrate. (a) Shows the spectrum distortion that occurs, especially at low energy, due to charging on the pad. (b) Shows the effect of adding 20 eV argon ions directed at the sample during Auger acquisition. From Ref. [12].

the net sample current, their use will be less successful as charge accumulation occurs beneath the surface. As the primary-electron energy increases, charge accumulation can occur deeper into the sample and one may expect the use of low-energy ions to neutralize the surface charge less effective as subsurface charge accumulates. Therefore, the effectiveness of low-energy ions for stabilizing the surface potential will likely be different for different electron beam energies, different electron incidence angles, and change for larger total electron doses. The example shown in Fig. 5 involved a 5-keV primary electron beam that was normally incident on the sample surface.

Many aspects of low-energy ion-beam “neutralization” are not well understood, and the technology will likely improve as users gain experience. For example, the method sometimes has a persistence effect in that the stability lasts after the ions are turned off [10,24]. Nonetheless, low-energy ions (that produce minimal sputtering) have been shown to be very effective at minimizing surface charging associated with conducting regions in a non-conductive matrix, as commonly found during analysis of integrated circuits and other advanced materials.

### 3.2. Sample thinning

It has long been recognized that enabling the incident electron beam to penetrate a thin insulating film on a conducting substrate can reduce or eliminate charge build-up [5,25,26]. The critical condition occurs when the penetration depth of the inci-

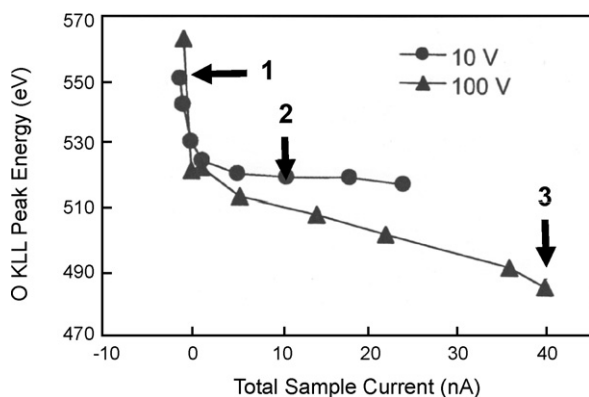


**Fig. 4.** Oxygen KLL Auger electron data collected on a PHI 700 Scanning Auger Nanoprobe [23] on a gold-plated bonding pad isolated from ground with a resistance greater than 500 M $\Omega$ . This system also uses a low-energy argon ion source to assist control of the surface potential. To establish the conditions for stable surface potential the energy of the ion beam was varied from 10 to 100 eV and the ion current from 0 to 40 nA. The incidence angle of the electron beam was 30° from the sample normal, the electron beam energy was 5 keV and the beam current was 5 nA. The ion gun was 45° from the sample normal. The AES O KLL peak position is at a stable energy for ions of 10 eV and for currents between 5 and 25 nA. Operating the ion gun at 10 V and 10 nA is reasonable for these conditions. From Ref. [11].

dent electrons exceeds the thickness of the insulating layer. The critical sample thickness will be material dependent (as discussed later), but for many materials it is typically hundreds of nanometers. It is frequently possible to analyze highly insulating layers grown on a conducting substrate as long as the incident electron beam penetrates the insulating layer, as schematically shown in Fig. 7. These thicknesses are also in the range of those used for specimens in TEM and it might be expected that the methods used to prepare TEM samples might also be useful for AES. Yu and Jin [27] have applied Ar<sup>+</sup> ion sputtering/dimpling and coating of the backside of the sample with a conducting metal film to prepare films for AES analysis, and have noted the effectiveness of this procedure in enabling analyses of complex modern high-performance ceramics.

The development of focused ion beams also allows the creation of very thin films from larger samples, which may then be mounted on or supported by the thin carbon grids used in TEM analysis. Wannaparhun et al. [9] and Tsutsumi et al. [10] have effectively used the new focused ion beam (FIB) approaches for preparing TEM samples of selected areas to prepare samples for AES analysis. Wannaparhun et al. [9] have calculated the electron interaction depth ( $R_e$ ) (related to what Yu and Jin call the electron interaction volume) for various industrial oxides to estimate the maximum sample thicknesses that would allow electron penetration through a thin film. Fig. 8 shows the calculated values of  $R_e$  for four oxides at an incident electron energy of 5 keV. The thicknesses required to minimize charging (thinner than  $R_e$ ) for these materials are less than 200–500 nm at a primary energy of 5 keV. (We note that many researchers prefer to work at 10 keV which has somewhat larger  $R_e$  values.) Tsutsumi et al. [10] recommend thicknesses of about 100 nm (0.1  $\mu$ m) which would apply to many materials and is consistent with the calculations of Wannaparhun et al. [9]. Samples can be prepared in the manner now commonly used for TEM sample preparation involving the selection of an area for analysis, protecting a region with a metal deposit, using the ion beam to create a thin section and using a probe to remove the thinned region. Samples are frequently transferred to a conducting TEM grid. This approach not only minimizes charging but also decreases the AES signal from backscattered electrons and can thus increase the spatial resolution of the measurement [10]. These methods may be particularly useful for examining nano-structured materials where selected regions can be prepared for analysis and some of the background or interference impacts of other materials can be removed or minimized.

All of the methods used to produce thin insulating layers can be applied to minimize charging during AES analysis. However, in the application of these methods there are significant issues related to damage that an analyst must consider. Papparazzo [28] observed in a comment on the Yu and Jin work that the dimpling and sputtering process to produce a thin film can damage some types of materials. Sample handling during the thinning process may introduce contamination (C or other) that may mask the information being

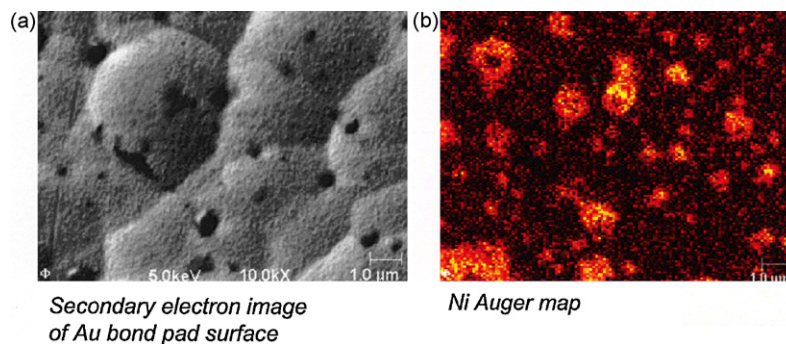


**Fig. 5.** (a) Secondary electron image of the Au bond pad surface from Fig. 4 and (b) Ni Auger map showing Ni islands on the bond pads. Data were collected during operation of an argon ion gun operated at the 10 V and 10 nA, noted as condition #2 in Fig. 4. From Ref. [11].

sought. In some cases ion sputtering was used to remove some contamination before elemental analysis. Use of FIB may introduce  $\text{Ga}^+$  into the sample which may interfere with the detection of other elements and the sputtering process will introduce some structural damage to the outer layer of the sample. Such damage is observed by TEM studies and can be minimized by finishing or polishing the samples using lower energy  $\text{Ga}^+$  ions. With the dimpling and  $\text{Ar}^+$  sputtering method, it is possible to thin the sample from one side, thereby minimizing sputter-damage effects, but concerns about carbon or other contamination on the outer surface would remain. The outer-surface contamination, however, may be beneficial in reducing charging.

Although damage issues must be considered, in many circumstances sample thinning does not destroy the information needed and the approaches can be very effective, especially for obtaining high-resolution data from complex materials or materials with complex structures. In some sense these approaches are related to angle lapping or other methods used to “polish” or otherwise prepare a sample for AES analysis. The FIB approach (along with  $\text{Ar}^+$  cross-section ion milling [29]) generates, by sputtering, a new surface that is perpendicular to the original surface, unlike that in normal depth profiling. Such sputtering methods are very effective at exposing the inner parts of a sample for in-depth dimensional analyses. These cross-section methods can allow high-resolution images and chemical analyses of conducting and insulating structural features not readily observed by other methods. An SEM image and related AES spectra from a semiconductor specimen thinned by the FIB process are shown in Fig. 9 [10]. Similarly, it is possible

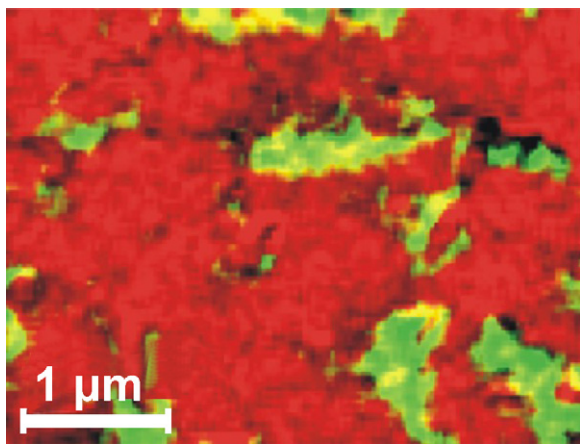


**Fig. 6.** Overlay of two scanning Auger maps from a ceramic surface acquired on a Thermo MICROLAB 350 [23] with 20 eV argon ions for charge compensation (red = nitrogen, green = oxygen) [12]. Without the low-energy argon ions, useful SEM images and SAM maps could not be acquired. (For interpretation of the references to color in this figure legend, the reader is referred to the web version of the article.)

to image the structures and different phases of complex high-performance ceramics [30].

#### 4. Methods for minimizing charging during AES

Many of the methods that have been effectively used to minimize charging effects (charge accumulation) during AES are summarized in this section. While the close relationship between sample charging and sample damage has been highlighted earlier, it must be noted that some of the methods used to address charging may themselves introduce damage or the potential for damage, and an analyst must be aware of these concerns.

The framework for considering approaches to reduce specimen charging was outlined in Section 2. In particular, the methods are discussed in three groups: (i) those which decrease sample resistance to ground or increase capacitance; (ii) those which adjust the total current to the sample; and (iii) those which adjust or optimize the TSEY.

##### 4.1. Decreasing sample resistance to ground or increasing capacitance

A variety of different methods can be used to lower the sample resistance to ground or increase the capacitance of the sample (Table 3), both of which can lower the surface potential (Eqs. (1) and (2)). The thinning approach mentioned as a current development is a specific case of the general method. These approaches are usually applied during the preparation or mounting of a specimen, and are not easily applied after a sample is inside a spectrometer.

##### 4.1.1. Decreasing the sample thickness (or effective sample thickness)

Decreasing the sample thickness lowers the total resistance of a poorly conducting material to ground which decreases any charging

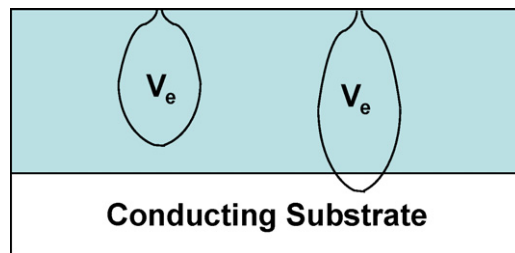


**Fig. 7.** Schematic drawing showing the electron interaction volume ( $V_e$ ) in an insulating film on a conducting substrate for different conditions. When the interaction volume of the incident electrons extends to a conducting substrate, charging of the insulating layer is decreased. This may be achieved by thinning a sample or by increasing the electron beam voltage.

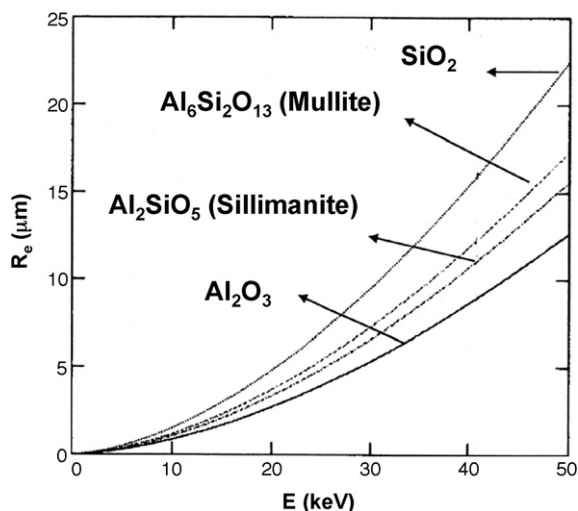


**Fig. 8.** Calculated values of the electron interaction depth ( $R_e$ ) for different compounds as a function of the primary-electron energy ( $E$ ). After Wannaparhun et al. [9].

potential (Eq. (1)). Decreasing the sample thickness of a highly insulating material increases the sample capacitance, thereby lowering the surface potential (Eq. (2)). In either circumstance, decreasing the sample thickness can have useful effects. This can be accomplished effectively by (a) using a coating, mask or other method to provide a shorter conduction path to ground to decrease the effective distance between the surface being probed and ground or (b) by actually thinning the sample in some way. It is useful to remember

that surface conduction may provide a good conduction pathway in many circumstances even when the bulk resistivity is high.

**4.1.1.1. Conduction paths—masks, meshes, coatings and deposits.** One of the most common methods that is attempted to minimize problems with specimens expected to have charging difficulties is to reduce the distance between the area irradiated by the incident electron beam and a conductor connected to ground [5,7,13,14]. This general approach can take many different forms depending on the nature and size of the sample and resources available to the analyst. Reducing the resistance of a sample to be analyzed to ground might be accomplished by placing a mask or grid around the region of interest during specimen mounting. It is also possible to temporarily cover the region to be analyzed and coat the remainder of the sample with a conducting layer. If the outer surface is not the primary region of interest, the whole specimen may be coated and a portion of the coating removed by sputtering [13,15,31]. Insulating particles may be deposited or pressed into a conducting substrate [13]. The interfaces of thin but insulating polymer layers on a conducting substrate have been prepared by coating the layer with gold, creating a tapered section by ball cratering (or using another polishing method) a cryo-cooled sample [32]. In the resulting tapered section, the polymer is the only non-conductor and charge build-up during analysis is minimized. Regardless of the preparation method, the overall sample mounting objective is the same. When AES spectra can be collected near the region of a conducting path to ground, the resistance between the surface being examined and ground is minimized, and surface charging can often be avoided. Although this approach can lower the resistance of the sample to ground, the same mounting procedures are also likely to

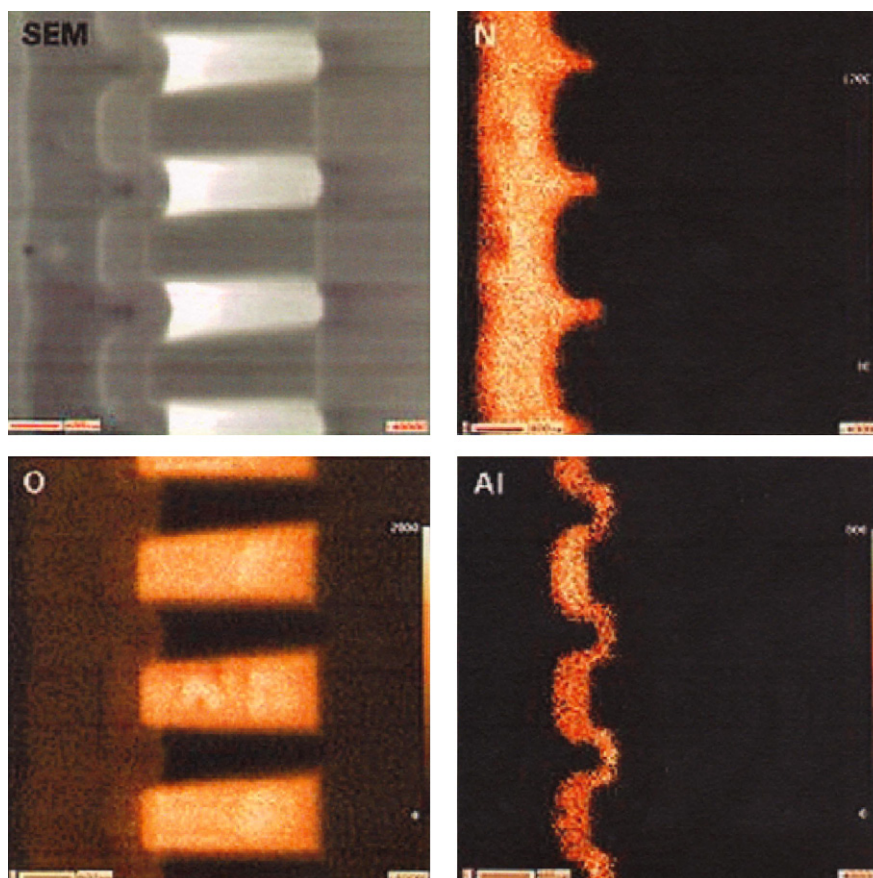


**Fig. 9.** SEM image and Auger N, O and Al maps from a semiconductor specimen prepared by the thin film method. Sections that are composed of SiO<sub>2</sub> or Si<sub>3</sub>N<sub>4</sub> can be analyzed, imaged and mapped without distortion. From Tsutsumi et al. [10].

increase the capacitance of the sample which will also be helpful in lowering the surface potential.

The advent of FIB or electron-beam-stimulated chemical vapor deposition provides a new way to provide a conductor close to a region of interest. A metal can be deposited on the surface of interest [33] inside a FIB/SEM. By depositing Pt “wires” on a printed circuit board, it was possible to analyze materials in regions isolated from ground using AES without the normal charging difficulties.

**4.1.1.2. Thinned samples.** Samples may be thinned in a variety of ways, either as they are initially prepared or before analysis. The use of a FIB or other capabilities to thin a variety of samples has already been discussed. Creative methods of argon-ion sputtering for cross-section preparation [29] have introduced new and potentially useful approaches to thinning samples for AES analyses. Any degree of thinning may help decrease the surface charging, but if the samples can be thinned to less than the depth of primary-electron penetration or the electron interaction depth (Fig. 8), it is generally observed that no charging occurs. With these sample preparation procedures, care should be taken to prevent alteration of sample properties of importance to the desired analysis.

As already noted, it is necessary to consider the impact of any sample thinning on the information that is desired from the analysis in addition to any damage by the electron beam during AES analysis. Sample damage during thinning might include oxide reduction and the creation of an amorphous or damaged layer with significant atomic rearrangement.

Samples created in thin-film form can be considered as a special case of a thinned sample, but deserve special mention. Analysis of many highly insulating materials can be accomplished with minimal charging if they can be created or grown as very thin films on a conducting substrate. Such samples are common in the electronics and sensor industries. In these cases, it is often useful to use an electron-beam energy high enough so that the beam penetrates the insulating layer to create a conduction pathway that minimizes charging [5,26] as shown in Fig. 7.

#### 4.1.2. Sample resistivity

Decreasing the sample resistivity can also be used to minimize or avoid sample charging [4,5]. This can be accomplished in several different ways depending on the sample including: adding impurities or dopants to the material (e.g., by ion implantation), UV irradiation, introducing radiation-induced defects, or heating the sample.

Although each of these approaches has been effectively used, they have significant limitations. Doping a material during film growth can create a conducting material if the doping does not alter other properties. The frequently studied rutile ( $\text{TiO}_2$ ) is often heated in a reducing environment to create oxygen vacancies and increase sample conductivity to allow examination [34]. The unexpected effects of this reduction on surface chemistry are becoming increasingly understood [35]. One common complication with specimen heating is surface segregation of material components or impurities.

Although it is common to think of altering overall sample resistivity to minimize charging, changes in surface resistivity and the detrapping of trapped charges are effective means of controlling the sample surface potential (even if the bulk resistance is not altered significantly). It should be noted that, in the discussion of the TSEY below, a steady-state condition can be established when the electron penetration depth is approximately equal to the secondary-electron escape distance [4]. In this zone of holes (created by secondary electron departure) and electrons, there is a good deal of charge mobility and it could be argued that this is a local decrease in resistivity.

#### 4.1.3. Strengths and limitations

Although thinning a sample can both lower sample resistance and increase capacitance, it may also be useful to recognize the important differences of these outcomes. When the sample resistance to ground is low enough to remove or minimize charge accumulation, the surface potential remains constant with time. A potential near zero will be a steady state, long-term condition, and AES analysis may be nearly as simple as for a metal. However, when the primary effect is to increase the capacitance, charge build-up will most likely still occur. The build-up of charge may be slowed long enough to allow the needed measurement, but (unless some other process intervenes) charge accumulation large enough to impact AES measurements will eventually occur.

Masks, sample thinning, and other approaches to enhancing sample conductivity are well worth trying and have been effective in many cases. However, researchers have also found the results to be disappointing for many samples where the methods appear inadequate for the needed task. This outcome may be likely to occur when the primary effect is not of lowering the resistance to ground, but of increasing the capacitance. The procedure may buy time for an AES analysis (or effectively a larger electron dose) before charging is significant but, if the analyst is expecting a longer time solution, this approach may not be adequate. It may be that the sample is sufficiently insulating that masking is useful, but other approaches (lowering the current density, optimizing the secondary-electron yield, or adding other charge sources) summarized below may also be needed.

#### 4.2. Optimizing the total secondary-electron emission yield

Several of the approaches commonly applied to minimize charging and allow data collection for a specific sample effectively involve efforts to optimize the total secondary-electron yield. The most common methods involve altering the primary-electron beam energy or the incidence angle of the beam (Table 4). Sometimes these approaches are tried without an analyst having a clear picture of the physical processes involved. To simplify the discussion, three different aspects of the TSEY are highlighted in the following three sections. Although these discussions differ in focus, they deal with different aspects of the same underlying physics. Understanding the full nature of TSEY is still an active area of research [16,36,37] and the discussion here is necessarily simplified.

##### 4.2.1. Conditions for general stability: energy, angle, electron dose, and contamination

Fig. 2 shows how TSEY ( $\sigma$ ) depends on the primary-electron energy ( $E_p$ ) and the primary-beam angle of incidence ( $\theta$ ) at the surface. The beam energy and incidence angle have traditionally both been varied to facilitate AES analyses of bulk insulators [38]. The maximum value of  $\sigma$  in Fig. 2 can range up to 25 for certain materials [8].

When  $\sigma > 1$ , the surface will develop a positive potential, while when  $\sigma < 1$  the surface will develop a negative potential (but a change of sign from positive to negative may occur during electron irradiation as noted below and in many references [16]). A positive surface potential of a few volts is sufficient to re-attract low-energy secondary electrons back to the surface, and to lower the total secondary-electron yield toward 1 while maintaining a relatively low surface potential. Conversely, the absolute value of a negative surface potential may grow to be very large, increasing with the incident beam energy eventually to approach the value of the accelerating voltage  $E_p/e$  of the primary electrons. If total charge neutrality cannot be obtained, this analysis suggests that positively charged surfaces will be more stable than negatively charged surfaces. The curves in Fig. 2 suggest that it will be easier to obtain the more stable positively charged surface at higher  $E_p$  as the incidence

angle of the primary beam increases. The experimental results of Seah and Spencer [21] generally verify this expectation for a range of clean and well-characterized insulators.

The secondary-electron yield will vary depending upon the composition of the sample, sample history, the experimental configuration, the vacuum conditions, and the presence of any surface contamination [5,39]. For example, carbon has been shown to decrease the TSEY and enhance the negative surface charge build-up [5,40,41]. Geller has shown that removal of surface carbon (using CO<sub>2</sub>) on MgO significantly enhanced charge dissipation [41]. Sample cleaning is not a universal solution, however, as in some circumstances sample cleaning from solvent cleaning or short durations of ion sputtering has been observed to increase charge build-up. If surface contamination enhances electron conduction along the surface, cleaning the sample may increase charge build-up. Therefore, for most samples, the presence or absence of charging along with approaches to minimize it should be determined during the analysis for the experimental conditions actually used. Some inconsistencies in the literature regarding TSEY values are probably due to differences in surface carbon contamination.

The analysis presented here and other related data support the value of a slightly positively charged surface. However, Seah and Spencer [18] also reported data that demonstrate limitations of this model due to charge accumulation below the surface. In addition to measuring the short-term surface potentials for various conditions, which appeared almost instantaneously, Seah and Spencer examined the longer term stability and frequently observed a high-dose longer time effect. They summarized the data collected for each material in a relatively simple diagram that presents useful combinations of primary-beam energy and incidence angle for specific materials. Their low- and high-dose stability diagram for silicon nitride is shown in Fig. 10 as an example of the considerations relevant for AES analyses of insulating materials. This figure demonstrates that silicon nitride did not initially show significant charging for beam energies below 5.2 keV (for normal beam incidence). As the total electron dose increased, however, charging did occur. At beam energies of around 2 keV, no charging effect was observed regardless of dose. Any deposited charge could persist for months, even when the surface potential was stabilized.

Seah and Spencer [21] found that the critical energy,  $E$ , and incidence angle,  $\theta$ , for which low-dose charging could be observed

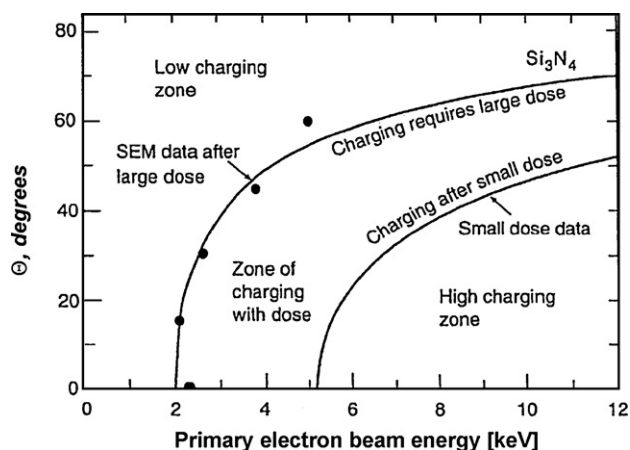


**Fig. 10.** Low- and high-dose stability diagram for Si<sub>3</sub>N<sub>4</sub> showing the regions of low charging and high charging for different combinations of primary-beam energy and angle of incidence,  $\theta$ . In the low charging zone, no charge build up was observed regardless of electron dose. For measurements in the high charging region, charging was observed almost instantly. The region between the two does not charge immediately but will show charging given sufficient electron dose. After Seah and Spencer [21].

was defined by a curve, drawn for Si<sub>3</sub>N<sub>4</sub> in Fig. 10, with the form  $E^{0.6} \cos \theta = N$  (where  $N$  is material specific and  $N = 2.7$  for Si<sub>3</sub>N<sub>4</sub>). The higher the value of  $N$ , the higher the energy for which the material will be stable for AES analysis. Seah and Spencer's data [21] for different materials suggest that the form of the equation represents general behavior of insulating materials but the particular value of  $N$  will depend on the instrument and the sample holder in addition to the sample material and any surface treatments.

The high-dose region in Fig. 10 occurs when significant subsurface charge is accumulated in the bulk specimen to change the TSEY, the near-surface charge, and thus the surface potential [3,16]. The measurements summarized in Fig. 10 demonstrate the relationship between beam energy and incidence angle and total electron dose for stable AES analyses. These measurements also demonstrate the earlier comments that charging is a complex phenomenon which cannot simply be described by a single TSEY curve for a material. More details of the time evolution of TSEY can be found in the paper by Cazaux [16].

This discussion highlights the value of producing a slightly positive surface charge on the sample if full neutrality cannot be maintained. The conditions for stable AES analysis depend on the material and may change with time as charge accumulates below the surface. Although a positive surface charge may enable useful AES data to be acquired with many insulating materials, it may be necessary to use lower incidence energies than would be needed to obtain high lateral resolution. It should also be remembered that variations of primary-electron energy will change the relative elemental sensitivity factors and thus additional data may be needed for quantitative analyses.

#### 4.2.2. TSEY and self-compensated charge neutrality

There are two special conditions (as shown in Fig. 2) for which there is a balance between the incoming current and the total secondary-electron current (i.e., when  $\sigma = 1$ ). The lower energy,  $E_{p1}^0$ , (for a specified  $\theta$ ) at which  $\sigma$  is 1 as a function of increasing primary-electron energy ( $E_p$ ) is usually below the value of  $E_p$  for which there is a useful Auger electron yield. However, the upper value,  $E_{p2}^0$ , is often in an energy range appropriate for AES. As noted by Oechsner [8], near  $E_{p2}^0$ ,  $d\sigma/dE_p < 0$ , which has important implications. When  $E_p$  is slightly above  $E_{p2}^0$ , the sample will charge negatively and will decelerate electrons approaching the surface, effectively lowering  $E_p$  toward  $E_{p2}^0$ . If  $E_p$  is slightly less than  $E_{p2}^0$ , the surface will charge slightly positively and attract low-energy secondary electrons to the surface, again driving the net electron current towards zero. Therefore, when  $E_p$  is approximately equal to  $E_{p2}^0$ , the system is self-adjusting or self-compensated [4,8,21,42] and stable AES spectra can be collected (subject to limitations due to possible sample changes due to electron stimulated desorption, other damage effects and the charge accumulation below the surface).

This analysis nicely defines a region of primary energy and angle of incidence for which stable AES data can be collected and which is often very useful for analyses on real samples. There are, however, practical limitations of this approach that include:

- (i)  $E_{p2}^0$  may change for different locations on a sample leading to different stability conditions for these regions. This situation complicates data collection (especially for generation of elemental maps) and can lead to undesirable variations in sensitivity for Auger data collected in different regions. Analyses of complex multi-phase materials can thus be a challenge.
- (ii)  $E_{p2}^0$  may not be in the energy range for desired beam or analysis conditions (e.g., for materials where high spatial resolution is needed). In addition, adjustment of the beam energy for a spe-

cific sample or a specific location on a sample may not allow easy comparisons of Auger data with similar data for other regions of the sample or from different materials for which the TSEY and  $E_{p2}^0$  were significantly different. Note that  $E_{p2}^0$  may often be increased (moved to higher energy) by tilting the sample. However, as shown in Fig. 2, if  $\sigma$  does not drop below 1, there is no  $E_{p2}^0$  and the approach can no longer be applied.

- (iii) Although very useful in a variety of circumstances, the selected conditions can often be used only for a limited time because the approach ignores the effects of time, electron dose and electron penetration depth (as shown in Fig. 10). Effectively, the analysis assumes a static or constant behavior for  $\sigma$  as a function of  $E$ . For a variety of reasons, this is not usually the case [16].

#### 4.2.3. TSEY, time-dependent charge accumulation and conditions for long term stability

A systematic effort to understand and model TSEY curves has been described by Cazaux [3,4,16] and used to explain a wide variety of phenomena reported by different researchers. A TSEY curve characteristic of an insulator is shown in Fig. 11. Features that differ from those typical of metals include a significantly higher initial maximum value of  $\sigma$  and the movement of  $E_{p2}^0$  to higher energies.

Several different values of the primary energy have been identified in the discussion so far and they are listed here for clarity along with definitions of two additional energies,  $E_p(\text{max})$  and  $E_{p2}^c$ :

- $E_p$  = energy of the primary or incident electron beam;
- $E_p(\text{max})$  = primary energy at which the TSEY is a maximum;
- $E_{p1}^0$  = lower primary energy at which  $\sigma = 1$ ;
- $E_{p2}^0$  = upper primary energy at which  $\sigma = 1$ ;
- $E_{p2}^c$  = primary energy at which the electron interaction depth ( $R_e$ ) or range of incident electrons is approximately equal to the maximum escape depth of the secondary electrons. Typically,  $E_{p2}^c$  is higher than  $E_p(\text{max})$  and lower than  $E_{p2}^0$ .

The dashed curve in Fig. 11 schematically represents the TSEY on a surface without the build-up of sub-surface charge. The solid line provides a schematic illustration of how the TSEY can change with time as charge accumulates near the surface. Understanding the time dependence of charging processes requires paying special attention to whether  $E_p$  is close to  $E_{p1}^0$  or  $E_{p2}^c$  and the fact that charging is a three-dimensional phenomenon that occurs in the near-surface region of the sample and not simply at the surface.

As summarized by Cazaux [4,16,21] and shown pictorially in Fig. 11, different charge distributions form as a function of time

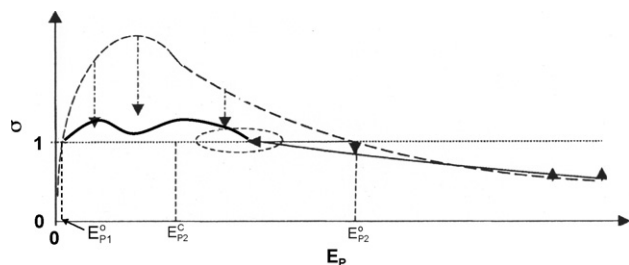


**Fig. 11.** Highly schematic drawing of the types of time-dependent changes expected in the TSEY ( $\sigma$ ) as a function of the primary energy  $E_p$  for a given total electron dose. The dashed line shows the initial TSEY and the solid line shows the TSEY curve as it evolves after a given dose of electrons. There is a much more rapid decrease in  $\sigma$  when  $E_{p1}^0 < E_p < E_{p2}^0$  than the rate of increase when  $E_p > E_{p2}^0$ . There is also a slow decrease in the energy at which  $\sigma = 1$  (the circled region) toward  $E_{p2}^c$ . Based on drawings of Cazaux [3] and data from Hoffmann et al. [36].

depending upon the energy of the primary beam  $E_p$  in relation to the other energies listed above and the total incident electron flux. If  $E_{p1}^0 < E_p < E_{p2}^c$ , the surface will charge positively to a depth approximately equal to the penetration depth of the incident electrons because more negative charges leave the surface than arrive. As charge builds up, the number of emitted secondary electrons will decrease since fewer low-energy electrons can escape. If  $E_{p2}^c < E_p < E_{p2}^0$ , the surface will initially charge positively, because of the loss of secondary electrons, but primary electrons travelling deeper than the secondary electron escape depth will also cause a negative charge build-up below the surface. This charge will increase with time, setting up a near-surface dipole layer and possibly leading to a net negative charge over time. As charge builds up, the effective TSEY will change with time and the effective  $E_{p2}^0$  will shift toward  $E_{p2}^c$ , as indicated by the circled inflection point in Fig. 11. When  $E_p \approx E_{p2}^c$ , the near-equality of the penetration depth of the primary electrons and the escape depth of the secondary electrons permits rapid recombination of electrons and positive charges in the same layer and a steady-state condition can be established. Here  $eU_s \approx E_p - E_{p2}^c$  (where  $e$  (the electronic charge) and  $U_s$  are both negative). If  $E_{p2}^0 < E_p$ , the surface and near-surface regions will be negatively charged although the charge build-up will slowly increase the secondary yield toward  $\sigma \approx 1$ .

A major implication of this analysis of the time and depth-dependent charge build-up is that a long-term stable condition can be achieved when  $E_p$  is less than but nearly equal to  $E_{p2}^c$ . This condition occurs when the range of the primary electrons is roughly equal to the escape depth of the secondary electrons. The condition is dependent on the angle of incidence of the primary electrons since the penetration depth decreases as electrons are incident on the sample at more glancing angles, effectively moving  $E_{p2}^c$  to higher energies. The resulting value of  $E_p$  may not be as large as desired for some high-resolution AES measurements, but may work well in many situations. We also note that for some conditions a surface will initially charge positively (and be useful for analysis) but will become negative as the electron dose increases, as discussed by Cazaux [16] and demonstrated by the Seah and Spencer data [21] shown in Fig. 10.

There are circumstances when it is desirable to use electron energies above  $E_{p2}^c$  or  $E_{p2}^0$ . By sample thinning, multiple beams, dose limitations, or other means, satisfactory AES measurements at higher beam energies may be possible. Since primary electrons with energies between 5 and 25 keV can penetrate the sample to depths up to a micrometer, there will be both charge movement through material below the surface and, for good insulators, charge accumulation. Charge accumulation below the surface and the surface potential it induces will eventually have an impact on AES measurements as analyzed theoretically by Cazaux [3,4,18] and demonstrated by the Seah and Spencer work [21]. There are three different physical processes that produce time-dependent behavior. First, the build-up and change of surface potential can occur very rapidly (i.e., on the time scale needed to acquire an AES spectrum) [4,21]. Second the build-up of subsurface charge changes the surface potential which in turn changes the TSEY, generally over longer times depending on the sign of  $U_s$ . Because of these two different time scales for charging effects, it can be important to minimize total exposure to the electron beam. The third effect is sample damage or induced diffusion in the sample due to the build-up of the electric field. The depth over which sub-surface charge build-up occurs increases (for bulk specimens) as the beam voltage increases.

Although charge transport into the sample may cause difficulty for AES analyses of "thick" insulating materials it provides a tool for analysis of thin samples as discussed earlier.

#### 4.3. Reducing the current density, limiting primary-electron dose, and additional current sources

The net or sum of all currents to and from the sample controls the sample potential as shown by Eqs. (1) and (2). The optimization of effects associated with the TSEY, as just discussed, is one method of adjusting the total current to and from the sample. There are a variety of other methods (Table 5) to control the current for highly resistive materials and also for samples isolated from ground. These methods fall into two categories: (a) those involving adjustment of the primary-electron beam incident on the sample and (b) those that involve an additional source of current to or from the sample. An analyst usually has control over the incident electron beam and can easily make some adjustments. As observed for the use of low-energy Ar<sup>+</sup> irradiation discussed earlier, the application and availability of other current sources will depend on the instrument configuration. Much of the motivation for adding a second source of sample current is the desire or need to perform AES analyses with high lateral resolution.

##### 4.3.1. Electron beam current density

Among the controls easily accessible to an analyst are the primary-beam energy, current, and current density. Changing the beam energy has already been discussed in the context of the TSEY. As already suggested, it has also been found useful in some circumstances to reduce the primary current [5]. This method can be helpful if the sample resistivity is marginal for satisfactory AES measurements and longer analysis times are feasible (i.e., the sample is considered as a capacitor). A critical issue then is whether enough data can be collected in the available time for the experimental objectives. Lowering the current density can be accomplished by defocusing or rastering the electron beam. Although beam rastering can work in some circumstances, Cazaux [4] observed that rastering of a focused beam can lead to some of the problems described in the previous section and is not as effective as using a defocused beam in reducing charging. Seah and Spencer [21] showed, for example that, for some sample conditions, important aspects of charging were independent of beam-raster size. We also note that use of a rastered or defocused beam has the obvious disadvantage of decreased lateral resolution, a major problem if high-spatial-resolution information is needed.

##### 4.3.2. Total primary-electron dose

The time dependence of the TSEY discussed above [4] and the data of Seah and Spencer [21] highlight the effect of total electron dose to the sample. At least two different charging mechanisms are relevant. One occurs almost immediately (due to charge accumulation on the outer surface) and appears to be nearly independent of the primary-beam current density. The other charging mechanism depends upon the total dose of primary electrons on the sample and is, therefore, time-dependent. A sample that first charged positively may eventually charge negatively as the total dose increases. This type of behavior shows that limiting the total electron dose to a specific part of a sample can be an important analysis strategy. This approach applies both to imaging of the sample and to collection of spectral data.

It is also important to remember that the amount of electron-induced desorption from a surface (and related sample damage) will also be dependent upon the total dose of primary electrons (and possibly other charge sources) on the sample. Tables of dose thresholds for 10% change in signal have been published by Pantano and co-workers [43,44].

##### 4.3.3. Use of additional current sources (irradiation by ions, electrons or photons)

The net current to the sample can be altered by providing an additional source of current. The use of low-energy ion beams to neutralize or at least stabilize the surface potential is one of the newer and seemingly powerful advances that are taking place for charge compensation during AES analysis, as discussed above.

Low-energy electrons have been found useful for producing a surface potential close to zero in some circumstances [5,6]. The energies of the electrons used vary from a few eV to as much as 400 eV [6]. These low-energy electrons can compensate the charge on a positively charged surface and produce additional secondary electrons on a negatively charged surface [5,21]. In concept, low-energy electrons can optimize the TSEY to control the surface potential (producing a net  $\sigma > 1$ ) while higher energy electrons are used for analysis. This dual-beam approach allows the higher energy focused beam for analysis while the lower energy beam controls the surface potential. One challenge of using a  $\approx 400$  eV electron beam for charge compensation is the presence of an elastic peak [6] from this source that could potentially overlap other peaks in an Auger spectrum. This approach does not appear to be widely applied.

Ion sputtering and irradiation with ultraviolet light can increase the number of charge carriers within an insulating sample and near the sample surface. Any mobile charge can help neutralize charge build-up, but other processes such as ion damage or photo-induced reactions may alter the sample causing potential complications for AES analysis and for the experimental objectives.

##### 4.3.4. Vacuum conditions and gas additions

Ambient background gases in a vacuum system can impact charging and gases may sometimes be deliberately added to minimize charging and/or decrease beam induced sample damage. Ambient gases have been observed to alter the rate and extent of beam damage, be involved in beam induced carbon deposition on a sample, and influence the extent of charge build-up. For some oxides, the presence of low pressures of oxygen (or the use of ozone) minimizes electron-beam-induced reduction of the oxide, decreases the build-up of carbon from the ambient gas, and minimizes the accumulation of surface charge [45]. Other gases may similarly decrease charge build-up (as commonly observed in environmental secondary electron microscopes [46–48]) but such effects have not been extensively studied or reported for AES.

#### 4.4. Dealing with rough surfaces, particles, fibers and non-uniform samples

Many approaches and some analyses for dealing with charging are based on the assumption that insulating samples have a uniform composition and, in some cases, that the samples were thick relative to electron penetration depths. Such uniform samples are generally not of greatest interest for Auger analyses; instead, it is often desired to perform surface analyses on heterogeneous samples that can have complex morphologies and topographies. Bombardment of such surfaces with a focused electron beam will frequently lead to conditions in which the surface potential varies laterally along the surface, as described by Cazaux [3]. Gao et al. [45] found that AES peaks sometimes split into two and that these can be attributed to Auger electrons emitted from two regions on the sample surface, one being the center of the primary beam (with one surface potential) and the other being a region outside that irradiated by the primary beam (at a different surface potential).

The analysis of finely structured materials is often a high priority for AES analysis and the approaches discussed in the recent developments section may be applied to such samples. Particularly difficult are situations when local charging prevents the primary-

electron beam from analyzing the region of greatest interest. Although there are no general solutions, many useful approaches were developed, as described below, for specific types of samples before the availability of low-energy ion sources and the application of FIB for sample thinning.

Samples containing small insulating particles, fibers, or insulating samples with rough surfaces often exhibit differential charging during AES analyses. Clearly, it is much more difficult to control the local primary-beam incidence angle for such samples. Consequently for particles or powder samples sample mounting is often of considerable importance for successful analysis [49]. Jenett noted the difficulty and value of sophisticated techniques for sample preparation for particle analysis [50]. If the particles or fibers have sufficiently small diameters and can be mounted in a single layer on a conducting substrate, they can be treated as a thin film, and minimal charging may be observed for higher energies of the primary beam. It is often useful to press powders, particles, and fibers into a soft conducting metal such as indium, onto double-sided sticky conducting tape [7,13] or imbed them into a TEM grid. If the particles can be deposited in a thin layer on a carbon foil (such as a TEM grid), it may be possible for the primary beam to penetrate the particles; Auger and secondary electrons from the carbon foil will generally provide minimal background or interference to the AES spectrum from the sample [10].

Although not always carefully reported in publications, many researchers have developed their own detailed and successful methods for working with samples of importance to them. Issues to be considered include the potential of mounting procedure to produce signals that overlap spectral regions of interest of the sample, the tendency of mounting to alter the particles, the size and mechanical strength of the particles and the ease with which they can be handled. A description of mounting particulate materials in indium as implemented at the University of Surrey is described in some detail as one specific example of the issues and considerations that might apply. Embedding particles into a soft metal such as gold or more often indium has been useful for analysis of insulating particulate materials such as catalysts. This has been found to be easier to accomplish than imbedding particles in a periodic gold TEM mesh. Best results are obtained with clean (i.e. bright) indium foil and if the facilities are available it is best to roll the indium foil shortly before use, old foil will appear dull as a result of the air formed oxide layer and this may compromise the electrical properties and lead to ineffective charge bleed off. The thickness of the foil does not seem to be particularly important. Thicknesses around 100  $\mu\text{m}$  seem to work well. The approach is to cut a piece of foil approximately 10 mm  $\times$  20 mm and sprinkle a small amount (enough to ensure that particulate/particulate contact is established in the next stage) of the candidate powder on an area of about 10 mm  $\times$  10 mm. The foil is then folded over on itself so the particles are contained within the indium foil “sandwich”. The foil then needs to be pressed to embed the particles into the indium and various methods can be used to apply gentle pressure, sufficient to embed the particles but not to fracture them. Possible methods include a metallographic hand press, machine vice or judicious use of a lever press. The foil is then opened out and both side will have particulates attached, it is then a simple matter to cut a small sample (about 5 mm  $\times$  5 mm) for mounting on the sample stub for Auger analysis, ensuring electrical contact is achieved between the indium foil and the sample mount.

A few analysis approaches can also assist characterization of particles already mounted and in the spectrometer if charging remains an issue. It may be natural and useful to work with the minimum currents for which useful signals can be obtained. However, possibly because an electron beam can heat a small particle, Hock et al. found it easier to analyze fly ash particles with high beam currents in preference to the lower currents often utilized when charging issues are

of concern (since the conductivity of the particles increased after heating) [51]. For rough surfaces, Park recommends focusing the primary beam on the top of the most prominent protrusion [52].

Some of the newly developed techniques seem particularly useful for examining small features in samples containing both conducting and non-conducting regions. Samples with fine features, including those buried below the surface, can sometimes be identified and analyzed using a FIB and argon-ion cross-section sample preparation in combination with thinning or other charge-compensation approaches [9,10,42]. Because of damage and sputtering effects, the use of these thinning methods must be applied with caution. When the thin-film samples are mounted on a low-atomic-number support such as carbon (to minimize electron scattering), the effects of backscattered electrons on the achievable lateral resolution in AES are minimized [53,54]. The use of low-energy positive ions also appears quite effective in allowing analyses of conducting regions in a non-conducting matrix. Improved lateral resolution can then be achieved for both imaging and point AES analyses [10].

#### 4.5. Depth profiling

The use of AES in combination with ion milling to obtain sputter depth profiles of the near-surface region of many types of materials, including poorly conducting materials, has been one of the major applications of the technique. One early such application was the measurement of sputter depth profiles of weathered or corroded glasses [55,56]. Researchers routinely used the range of methods described above to minimize charging when profiling bulk or thick films of the glasses. During sputter profiling, the samples were commonly tilted (so that the primary beam was at more grazing incidence) and were bombarded by low-energy electrons to stabilize the surface potential and the AES signals [55]. It might seem concurrent irradiation with positive ions could help stabilize the surface. However, the situation can be complex. Borchardt et al. [42] and many others note that ion sputtering can perturb the surface and near-surface charge build-up that would normally occur during AES analysis of an insulator (as described above), and the overall effect on surface potential and compositional stability is difficult to assess.

Many studies have been made on the perturbing effects of both electron [43,44,56] and ion [57,58] beams on glass and mineral surfaces (e.g., alterations of near-surface composition and other properties). In spite of possible charging and damage complications, researchers routinely have been able to collect informative AES profiles of glasses and other insulators. It has also been possible to study the extent to which the primary beam induces elemental migration [26,59].

Although the combination of AES and sputtering of insulators is relatively common and often very informative, it is frequently not routine. Consequently, several additional approaches have been used to enhance the reliability and sometimes the speed of collecting composition information as a function of depth into the material. In some cases, ion sputtering (as well as polishing as noted earlier [32]) has been used to open a tapered or angled surface exposing a cross-section of the surface region that was then examined by AES analysis of the exposed surface. One research group found that this approach was advantageous over the traditional sputter-profile method [60]. The extraction of thin samples using FIB technology will also facilitate cross-section depth profiles [9] and represents a new approach for obtaining depth information by AES.

While measurements of depth profiles for “bulk” insulating materials can be challenging, sputter profiles can often be measured of thin insulating films on conducting substrates (e.g., corrosion layers) and sometimes benefit from the increased primary-energy

approach described earlier [26]. Covering an insulator surface with a metal coating before sputtering might be considered a special case of the aperture or mask approach described earlier, but has proved useful in some circumstances [31].

When high-spatial-resolution is required, charge build-up in the sample may cause the beam position to shift. Some type of image registration or position adjustments may be needed in such cases.

## 5. Summary

Many useful approaches have been developed for collecting AES data from insulating material and conductors isolated from ground. The physical understanding of the relevant processes is well established for many of these methods. Understanding the physical principles can help an analyst to optimize an approach or to select the easiest method to apply. Tables 1–5 are provided to assist this process.

New experimental capabilities (the availability of low-energy (<20 eV) ion sources and FIB-based sample thinning) facilitate the application of methods that enable AES analyses with high spatial resolution on samples or material systems that were previously impossible to analyze. It is now feasible to obtain elemental maps for complex ceramics and to analyze insulating as well as isolated metallic regions on complex semiconductor structures. The advantages of irradiating a sample with low-energy ions for charge compensation appear to be significant, but the challenges and limitations have not been fully explored.

For materials with marginal conductance to ground, various mounting and sample-preparation approaches can be used to facilitate stable conditions for AES analysis while the surface potential remains near-zero or at a constant steady value.

For electrically isolated portions of a sample or for highly insulating samples, a variety of methods can be used to facilitate AES analyses and to increase the time over which useful data can be collected. In many circumstances, however, sub-surface charge build-up will occur for longer analysis times (higher electron doses), and it is often necessary to minimize the analysis time.

For insulating materials it is particularly important to remember that electron beams (and some sample preparation methods) can modify the surface composition and/or chemistry of a material and that charge accumulation can lead to selective diffusion and elemental segregation. If an analyst is aware of these risks and they appear likely to impact the information to be collected, it is often possible to use approaches which avoid, minimize or correct for these effects.

## Acknowledgements

This paper evolved as a result of the development of ISO Standard “Surface Chemical Analysis – Auger electron spectroscopy – Reporting of methods used for charge control and charge correction” (ISO 29081) and the participation of many international experts in the preparation of this standard is gratefully acknowledged. As the project leader, DRB especially thanks the many researchers, vendor representatives, and ISO TC201 and ASTM E42 committee participants and members who have provided suggestions, data, comments, and ideas that were incorporated into the standard as well as this paper. Several very helpful discussions with J. Cazaux on how to present a simplified, but reasonably correct, discussion of TSEY are gratefully acknowledged. Part of the motivation for this effort derived from needs and experience of users working to characterize complex materials and nanostructures in the EMSL—the Environmental Molecular Sciences Laboratory, a U.S. Department of Energy (DOE) national scientific user facility located at the Pacific National Northwest Laboratory (PNNL). This work also supports

research programs sponsored by the Offices of Basic Energy Sciences and Biological and Environmental Research of the US DOE at PNNL.

## References

- [1] J. Cazaux, *J. Microsc.* 217 (2005) 16–35.
- [2] J. Cazaux, *Microsc. Microanal.* 10 (2004) 670–684.
- [3] J. Cazaux, *J. Appl. Phys.* 95 (2004) 731–743.
- [4] J. Cazaux, *Nucl. Instrum. Methods Phys. B* 244 (2006) 307–322.
- [5] S. Hofmann, *J. Electron. Spectrosc.* 59 (1992) 15–32.
- [6] S. Ichimura, H.E. Bauer, H. Seiler, S. Hofmann, *Surf. Interf. Anal.* 14 (1989) 250–256.
- [7] M.A. Kelly, in: D. Briggs, J.T. Grant (Eds.), *Surface Analysis by Auger and X-ray Photoelectron Spectroscopy*, IM Publications, Chichester, 2003, pp. 191–210.
- [8] H. Oechsner, *Thin Solid Films* 341 (1999) 105–108.
- [9] S. Wannaparhun, S. Seal, K. Scammon, V. Desai, Z. Rahman, *J. Phys. D: Appl. Phys.* 34 (2001) 3319–3326.
- [10] K. Tsutsumi, T. Suzuki, Y. Nagasawa, Effective methods to prevent charging in Auger electron spectroscopy, Application and Research Center, JEOL Ltd. [http://www.jeol.com/jeolnews/jeol\\_news601/News%20home/66/index.html](http://www.jeol.com/jeolnews/jeol_news601/News%20home/66/index.html).
- [11] Physical Electronics Application Note, “Bond Pad Surface Characterization with the PHI 700 Scanning Auger Nanoprobe” Physical Electronics USA, 18725 Lake Drive East, Chanhassen, MN 55317.
- [12] Thermo Fisher Scientific Application Note: 31001 “AES, SEM and SAM charge compensation”, Thermo Electron, Surface Analysis Instruments, East Grinstead, UK.
- [13] ASTM Standard E 1078-02, Annual Book of ASTM Standards, ASTM International, West Conshohocken, Pennsylvania, vol. 3.06, 2006, pp. 685–93.
- [14] ISO 18116:2005, Surface Chemical Analysis—Guidelines for preparation and mounting of specimens for analysis, International Organization for Standardization, Geneva, 2005.
- [15] ASTM Standard E 982-05, Annual Book of ASTM Standards, ASTM International, West Conshohocken, Pennsylvania, vol. 3.06, 2006, 685–693.
- [16] J. Cazaux, *J. Electron. Spectrosc.* (in this volume).
- [17] Y. Strausser, in: C.R. Brundle, C.A. Evans, S. Wilson (Eds.), *Encyclopedia of Materials Characterization: Surfaces, Interfaces, Thin Films*, Butterworth-Heinemann, Stoneham, MA, 1992, p. 310.
- [18] J. Cazaux, *J. Electron. Spectrosc.* 105 (1999) 155–185.
- [19] P.D. Townsend, in: R. Behrisch (Ed.), *Sputtering by Particle Bombardment II*, Springer, Berlin, 1983, p. 147.
- [20] G.W.C. Kaye, T.H. Laby, *Tables of Physical and Chemical Constants*, 16th Ed., Longman Harlow, UK, 1995, Ref. [5], <http://www.glenbrook.k12.il.us/gbssci/phys/Class/circuits/u9l3b.html> and <http://hypertextbook.com/physics/electricity/resistance/>.
- [21] M.P. Seah, S.J. Spencer, *J. Electron. Spectrosc.* 109 (2000) 291–308.
- [22] M.A. Kelly, P.E. Larson, *J. Vac. Sci. Technol.* A16 (1998) 3483–3489.
- [23] Certain commercial equipment and components are identified in this paper in order to specify adequately the experimental conditions. Such identification is not intended to imply recommendation or endorsement by the National Institute of Standards and Technology or the U.S. Department of Energy nor is it intended to imply that the equipment and components identified are necessarily the best available for the purpose.
- [24] Physical Electronics Application Note, “Using Low Energy Ions for Charge Neutralization in Scanning Auger Microprobes” Physical Electronics USA, 18725 Lake Drive East, Chanhassen, MN 55317.
- [25] D.M. Taylor, *J. Phys. D: Appl. Phys.* 11 (1978) 2443–2454.
- [26] F. Ohuchi, F.M. Ogino, P.H. Holloway, G.G. Pantano Jr., *Surf. Interf. Anal.* 2 (1980) 85–90.
- [27] L. Yu, D. Jin, *Surf. Interf. Anal.* 31 (2001) 338–342.
- [28] E. Paparazzo, *Surf. Interf. Anal.* 31 (2001) 1110.
- [29] See for example JEOL Cross Section Polisher SM-09010, <http://www.jeol.com>.
- [30] L. Yu, D. Jin, *Surf. Interf. Anal.* 31 (2001) 1112–1113.
- [31] J.-W. Park, A.J. Pedraza, D.H. Lowndes, *J. Mater. Sci.* 34 (1999) 1933–1942.
- [32] This process without the gold coating is summarized in J.M. Cohen, J.E. Castle, *Inst. Phys. Conf. Ser.* #93, vol. 1, chapter 5, 1988, pp. 275–276.
- [33] R.N. Rao, T.C.W. Sang, H. Younan, L.K. Foo, ICSE2004. Proc. 2004, Kuala Lumpur, Malaysia, IEEE 2004, pp. 86–89.
- [34] U. Diebold, in: A.W. Czanderna, C.J. Powell, T.E. Madey (Eds.), *Methods of Surface Characterization, Specimen Handling, Preparation and Treatments in Surface Characterization*, vol. 4, Kluwer Academic/Plenum Publishers, New York, 1998, p. 145.
- [35] M.W. Li, U. Hebenstreit, M.A. Diebold, D.R. Henderson, Jennison, Oxygen-induced restructuring of rutile TiO<sub>2</sub>(110): formation mechanism, atomic models and influence on surface chemistry, *Faraday Dis.* 114 (1999) 245–258.
- [36] R. Hoffmann, J.R. Dennison, C.D. Thompson, J. Albreten, *IEEE Trans. Plasma Sci.* 36 (2008) 2238.
- [37] E.I. Rau, E.N. Evstafeva, M.V. Andrianov, *Phys. Solid State* 50 (2008) 621–630.
- [38] J. Cazaux, *Scanning* 26 (2004) 181–204.
- [39] F. Le Pimpec, R.E. Kirby, F.K. King, M. Pivi, *J. Vac. Sci. Technol. A* 23 (2005) 1610–1618.
- [40] A. Dallos, K. Shapiro, B.A. Shaw, *IEEE T. Electron. Dev.* 39 (1992) 2611–2615.
- [41] J.D. Geller, *Supplement a la Revue Le Vide: science, technique et application* 275 (1995) 644.

- [42] G. Borchardt, S. Scherrer, S. Weber, *Fresenius J. Anal. Chem.* 341 (1991) 255–259.
- [43] C.G. Pantano, T.E. Madey, *Appl. Surf. Sci.* 7 (1981) 115–141.
- [44] C.G. Pantano, A.S. D'Souza, A.M. Then, in: A.W. Czanderna, T.E. Madey, C.J. Powell (Eds.), *Beam Effects, Surface Topography and Depth Profiling in Surface Analysis*, Plenum Press, New York, 1998, p. 39.
- [45] H. Gao, H.W. Maus-Friedrich, V. Kempter, Y. Ji, *J. Vac. Sci. Technol. A* 21 (2003) 1009–1016.
- [46] B.L. Thiel, *Surf. Interf. Anal.* 37 (2005) 939–941.
- [47] D.J. Stokes, S.M. Rea, A.E. Porter, S.M. Best, W. Bonfield, *Materials Research Society Proceedings Library*, 2001 Fall Symposium FF, paper FF6.5.
- [48] M.T. Postek, A.E. Vladár, *Microsc. Microanal.* 11(Suppl. 2), 2005 DOI: 10.1017/S1431927605504422 P 388.
- [49] P.A. Lindfors, in: A.W. Czanderna, C.J. Powell, T.E. Madey (Eds.), *Methods of Surface Characterization, Specimen Handling, Preparation and Treatments in Surface Characterization*, vol. 4, Kluwer Academic/Plenum Publishers, New York, 1998, p. 45.
- [50] H. Jenett, *Surf. Interf. Anal.* 12 (1988) 535–537.
- [51] J.L. Hock, D. Snider, J. Kovacich, D. Lichtman, *Appl. Surf. Sci.* 10 (1982) 405–414.
- [52] J.-W. Park, *J. Vac. Sci. Technol. A* 15 (1997) 292–293.
- [53] ISO/TR 19319: 2003. *Surface chemical analysis – Auger electron spectroscopy and X-ray photoelectron spectroscopy – Determination of lateral resolution, analysis area, and sample area viewed by the analyser*, International Organisation for Standardisation, Geneva, 1003.
- [54] C.J. Powell, *Appl. Surf. Sci.* 230 (2004) 327–333.
- [55] L.L. Hench, *J. Non-Cryst. Solids* 19 (1975) 27–39.
- [56] C.G. Pantano Jr., D.B. Dove, G.Y. Onoda Jr., *J. Non-Cryst. Solids* 19 (1975) 41–53.
- [57] M.F. Hochella, J.R. Lindsay, V.G. Mossotti, C.M. Eggleston, *Am. Miner.* 73 (1988) 1449–1456.
- [58] D.F. Mitchell, G.I. Sproule, M.J. Graham, *Surf. Interf. Anal.* 15 (1990) 487–497.
- [59] A.A. Glachant, *Thin Solid Films* 254 (1995) 54–60.
- [60] R.A. Chappell, C.T.H. Stoddart, *J. Mater. Sci.* 12 (1977) 2001–2010.